Collisionless Electrostatic Single-Probe and Double-Probe Measurements

E. W. PETERSON*
University of Minnesota, Minneapolis, Minn.

AND

L. TALBOT†
University of California, Berkeley, Calif.

An algebraic fit is made to the results of a numerical analysis describing the collisionless current attracted to cylindrical Langmuir probes whose ratios of probe radius to Debye length are of moderate value. The probe currents indicated by these expressions are compared to some numerically computed values and to values obtained using an approximate analytical solution. This algebraic description of the single-probe response is then used to derive the double-probe characteristics in the region where the current attracted to the probe is potential-dependent. Equations are derived and methods are discussed for accurately determining both electron temperature and number density from these double-probe characteristics. The analogous results for double-probe operation in the region of orbital-motion-limited current collection are also included.

Nomenclature

A = probe area
H = double-probe current
I = probe current (repelled species)
J = probe current (attracted species)
j = normalized current (attracted species)
J_0 = Eq. (2)
k = Boltzmann's constant
L = probe length
M = mass
N = density
q = one electronic charge
r = probe radius
T = temperature
V = applied probe-to-probe or probe-to-reference potential
Z = number of electron charges on particle
α = Eq. (5)
β = Eq. (6)
ϵ = Eq. (21)
θ = kT/Zq effective temperature (eV)
λ = $(kT/4\pi NZ^2q^2)^{1/2}$ Debye length
τ = $-\frac{1}{2}\ln(M_+/M_-)$
Φ = potential measured with respect to the plasma potential
χ = Φ/θ_- nondimensional potential
ψ = V/θ_- nondimensional applied potential

Subscripts

a,r = attracted, repelled
e,i = electron, ion
$+,-$ = colder, hotter
1,2 = numerical designation for double-probes
f = open circuit (floating) potential

1. Introduction

THE free-molecule cylindrical Langmuir probe is one of the most common diagnostic tools used for measuring the properties of plasmas and several[1-3] reviews of probe theory and application are available in the literature. As is well known, the slope of the logarithm of the electron current in the electron-retarding region is a measure of the electron temperature, whereas the electron density may be determined from a measure of the attractive-field probe current in a region where this current is theoretically well defined. Laframboise,[4] in numerically solving the theoretical analysis previously formulated by Bernstein and Rabinowitz,[5] has provided the required theoretical values for the current (ion or electron) attracted to a probe. His results are valid for a wide range of ratios of probe radius to Debye length (r/λ), a complete range of ion to electron temperature ratios (θ_i/θ_e), and have been experimentally verified in a variety of gases.[6-9] The numerical results obtained by Laframboise are presented in a manner suitable for use by the experimentalist, and the reduction of probe current data to plasma electron (or ion) density proceeds quite simple by following the method given by Sonin.[6]

However, various applications exist where an analytical description of the probe characteristics is required. For example, the floating double-probe may be used to determine electron temperature and density if its current voltage characteristic is given in analytical form. However, the derivation of the double-probe characteristic proceeds from an analytical description of the single-probe response. Consequently, the double-probe theory previously presented by Johnson and Malter[10] was necessarily limited by the restrictive assumption that ion current collection was independent of the probe potential. In addition, recall that the probe response to low-frequency fluctuations in the plasma properties is determined by perturbing the probe steady-state equations about the mean plasma properties; a procedure which obviously requires an accurate analytical description of the probe steady-state characteristics. In fact, the algebraic formulas presented herein were used in Ref. 11 to determine both the single-probe and double-probe transient responses.

Therefore the purpose of the present paper is to provide an algebraic description for the single-probe characteristics in the region where the Debye length is smaller than the probe radius, yet large enough so that the current attracted to the probe is potential-dependent. The values of probe current indicated by these expressions are compared to values calculated by Laframboise[4] and to values obtained using the approximate analytical expressions given by Kiel.[12] The floating double-probe characteristics are then derived using the

Received December 1, 1969; revision received March 30, 1970.

* Assistant Professor, Department of Aerospace Engineering and Mechanics. Member AIAA.

† Professor, Division of Aeronautical Sciences. Member AIAA.

Table 1 Numerical values of the constants appearing in Eqs. (5) and (6)

Constant	a	b	c	d	e	f	g	l	m
$(\theta_a/\theta_r) \leq 1$	2.900	2.300	0.070	−0.340	1.500	0.850	0.135	0.000	0.750
$(\theta_a/\theta_r) > 1$	2.900	2.300	0.110	−0.380	−2.800	5.100	0.135	2.800	0.650

algebraic expressions for the single-probe characteristics and the well-known expression for the electron current in the electron-retarding field region. Equations are derived and methods are discussed for determining the electron temperature and number density from the double-probe characteristics. The analogous results for double-probe operation in the region of orbital motion limited-current collection are also presented.

2. Single-Probe Analysis

The nondimensional current attracted to a probe may be expressed by

$$j = J/J_0 \tag{1}$$

where

$$J_0 = \pi r L Z q N (2kT_-/\pi M)^{1/2} \tag{2}$$

is the random thermal current which would be collected by the probe when the probe is at the plasma potential, if the effective temperature of the collected species were assumed to be that of the hotter species. Now the nondimensional ion current collected by an ion-attracting probe operating in the Vlasov limit with specified ratios of ion to electron temperature, probe potential to electron energy, and probe radius to electron Debye length is equal to the nondimensional electron current collected by an electron attracting probe having the same ratios of electron to ion temperature, probe potential to ion energy, and probe radius to ion Debye length. Therefore, the current attracted to the probe

$$j = j\{(\theta_a/\theta_r),\ (\Phi/\theta_r),\ (r/\lambda_r)\} = j\{(\theta_+/\theta_-),\ (\Phi/\theta_-),\ (r/\lambda_-)\} \tag{3}$$

may be written in terms of the "attracted" (a) or "repelled" (r) species or the "hotter" (—) and "colder" (+) species without further identifying them. A set of these nondimensional probe characteristics (j vs χ) has been computed by Laframboise[4] for a wide range of ratios of (θ_a/θ_r), and (r/λ_r).

It was found that this two-parameter family of characteristic curves could be closely reproduced by the algebraic relation

$$j = (\beta + |\chi|)^\alpha \tag{4}$$

where

$$\alpha = a/[\ln(r/\lambda_-) + b] + c(\theta_+/\theta_-)^m + d \tag{5}$$

$$\beta = e + \{f + g[\ln(r/\lambda_-)]^3 - [l/\ln(r/\lambda_-)]\}(\theta_+/\theta_-) + [l/\ln(r/\lambda_-)] \tag{6}$$

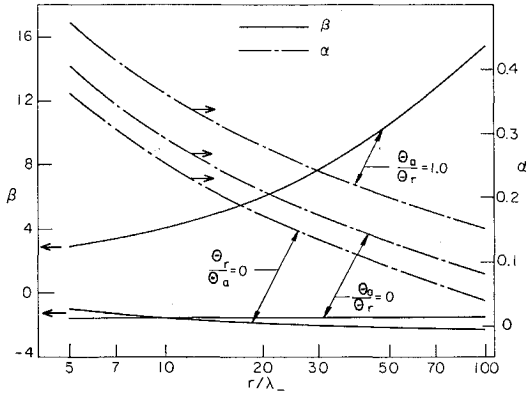

Fig. 1 Curve parameters.

$$\chi = \Phi/\theta_- \tag{7}$$

and where $[a\text{–}m]$ are numerical constants whose magnitudes are shown in Table I. Values of α and β are given in Fig. 1 as a function of r/λ_- for $\theta_a/\theta_r = 0$, 1, and ∞. Equation (4) is applicable for ratios of probe radius to Debye length (r/λ_-) between 5 and 100, and absolute values of the nondimensionalized potential $\chi > 3$ (>10) if $\theta_a/\theta_r \leq 1$ (>1), provided the assumptions underlying Laframboise's numerical analysis are also satisfied. Table II compares some typical values of probe current indicated by Eq. (4) with the numerically computed values given by Laframboise[4] and the values of probe current computed from the approximate analytical expressions (also valid for Debye lengths smaller than the probe radius) derived by Kiel.[12] As shown, both analytical expressions indicate values of probe current which differ from the numerically computed values by <3%.

It follows from Eqs. (1, 2, and 4) that once the electron temperature is known the density may be formally computed according to

$$N = J(\chi)/[AZq(\beta + |\chi|)^\alpha \theta_-^{1/2}(|Z_-|q/2\pi M)^{1/2}] \tag{8}$$

Since α and β depend slightly on density some iteration may be required to evaluate this relation. Recall, however, that Sonin[6] has demonstrated that the results given by Laframboise[4] may be used to construct universal graphs for a specified value of potential (e.g., $\chi_f - 10$). If the single-probe current $J(\chi_f - 10)$ is then measured, the number density and ratio of probe radius to Debye length may be obtained directly from such graphs.

3. Double-Probe Analysis

The double-probe characteristic such as the one shown in Fig. 2 may be theoretically derived using Eqs. (1, 2, and 4), and the well-known expression

$$I = Z_r N_r q A (kT_r/2\pi M_r)^{1/2} \exp(\Phi/\theta_r) \tag{9}$$

for the repelled species current by following a procedure similar to that used by Johnson and Malter.[10] To allow direct experimental interpretation of the results the dimensional probe current is considered for the common situation where $\theta_i/\theta_e \leq 1.0$.

Assume probes 1) and 2) having equal radii but with areas A_1 and A_2, respectively, are located in a plasma having con-

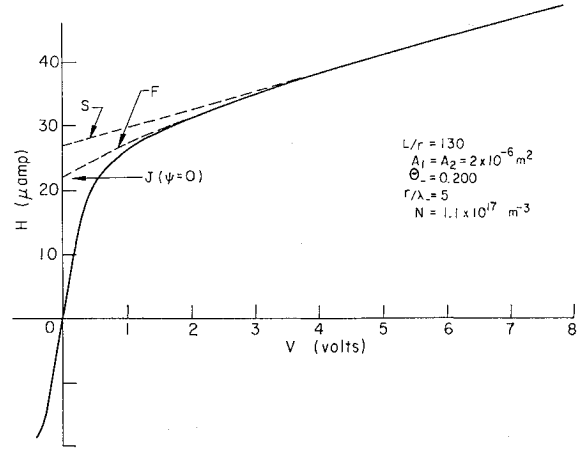

Fig. 2 Double-probe characteristic.

Table 2 Comparison of analytical and numerical calculations of probe current

χ	θ_+/θ_-	r/λ_-	$J_{+[\text{Eq. (4)}]}J_-$		$J_{+(\text{Ref. 4})}J_-$		$J_{+(\text{Ref. 12})}J_-$	
25	1.00	10	3.36	3.36	3.38	3.38	3.42	3.42
25	0.75	10	3.19	3.10	3.24	3.17	3.30	3.18
25	0.50	10	3.02	2.85	3.07	2.92	3.09	2.91
25	0.25	10	2.83	2.58	2.89	2.63	2.90	2.64
25	0.10	10	2.70	2.39	2.77	2.42	2.77	2.44
25	0.00	10	2.59	2.20	2.68	2.25	2.76	2.26
25	0.50	5	4.33	4.08	4.32	4.01	4.37	4.06
25	0.50	20	2.31	2.19	2.31	2.20	2.33	2.23
25	0.50	50	1.78	1.70	1.76	1.69	1.78	1.73
25	0.50	100	1.53	1.46	1.54	1.49	1.55	1.53
20	0.10	10	2.54	2.24	2.59	2.26	2.58	2.29
15	0.10	10	2.35	2.06	2.38	2.08	2.37	2.12
10	0.10	10	2.11	1.83	2.14	1.87	2.12	1.93
5	0.10	10	1.78		1.81	1.61	1.79	1.67
3	0.10	10	1.60		1.59	1.47	1.62	1.54

stant properties within the probe spacing. Then the current flowing in the double-probe circuit must be

$$H = J_1 + I_1 = -I_2 - J_2 \tag{10}$$

to satisfy the continuity requirement. Define the normalized value of the potential (V) applied between the two probes by

$$\psi = V/\theta_- = \chi_2 - \chi_1 \tag{11}$$

Now $\chi = \chi_f$ when $V = 0$, and therefore the normalized individual probe potentials may be written as

$$\chi_1 = \chi_f - \psi_1, \quad \chi_2 = \chi_f + \psi_2 \tag{12a}$$

where

$$\psi = \psi_1 + \psi_2 \tag{12b}$$

As illustrated in Fig. 3, ψ_1 and ψ_2 are the normalized values of the probe potentials measured with respect to the $V = 0$ (i.e., $\chi = \chi_f$) ordinate shown in Fig. 2. It follows from Eqs. (9, 10, and 11) that the double-probe characteristic is given by

$$H = [J_1(A_2/A_1)\exp\psi - J_2]/[1 + (A_2/A_1)\exp\psi] \tag{13}$$

where the ion currents (J_1,J_2) are found from Eqs. (1, 2, 4, and 12) to be

$$J_1 = J_{0_1}(\beta - \chi_f + \psi_1)^\alpha$$
$$J_2 = J_{0_2}(\beta - \chi_f - \psi_2)^\alpha \tag{14}$$

Recall that current continuity must be maintained. Thus the relative values of ψ_1 and ψ_2 are implied by Eq. (10). It follows, by using Eqs. (2, 9, 10, 12, and 14) as shown in Ref. 13, that ψ_1 is given implicitly by

$$\psi_1 = -\ln\{[1 + \psi_1/(\beta - \chi_f)]^\alpha + (A_2/A_1)[1 + \psi_1/(\beta - \chi_f) - \psi/(\beta - \chi_f)]^\alpha\} + \ln[1 + (A_2/A_1)\exp\psi] \tag{15}$$

where χ_f is the potential at which $J + I = 0$ and is found from Eqs. (1, 2, 4, and 9) to be given by

$$\chi_f = \tau + \alpha\ln(\beta - \chi_f) \tag{16}$$

while ψ_2 may now be found from Eqs. (12) and (15). Equations (13) and (14) represent the general form of the double-probe characteristic, and the analytical expressions given by Kiel[12] could equally well have been used for evaluation of $J_1(-\chi_f + \psi_1)$ and $J_2(-\chi_f - \psi_2)$ in the region where $r/\lambda_- > 5$.

The double-probe characteristic valid in the orbital motion limited regime, when the ion current collection is defined by Langmuir and Mott-Smith,[14] may be obtained from Eqs. (12, 13, 14, and 15) by putting $\alpha = \frac{1}{2}$, $\beta = 1.0$, whereas the thin sheath limit results of Johnson and Malter[10] may be recovered by putting $\alpha = 0$.

When the ion current collection is independent of potential (thin sheath limit) the electron temperature was shown[10] to be proportional to the slope of the double probe characteristic and the magnitudes of the ion currents all evaluated at $V = 0$. Similarly it can be shown,[13] using Eqs. (1, 4, 11, and 13), that the electron temperature measurement is

$$\theta_-(1 + \epsilon)^{-1} = \{[J_1J_2/(J_1 + J_2)](\partial H/\partial V)^{-1}\}_{V=0} \tag{17}$$

where

$$\epsilon = \alpha/(\beta + |\chi_f|) \tag{18}$$

and where χ_f is given by Eq. (16). Now the product $\theta_-(1 + \epsilon)^{-1}$ may be computed, according to Eq. (17), from the slope of the double-probe characteristic and the magnitudes of the ion currents (J_1 and J_2) all evaluated at $V = 0$. However, even though ϵ and χ_f are functions of r/λ_-, θ_+/θ_- and M_+/M_-, the value of ϵ as shown in Fig. 4 depends only slightly on electron temperature. Therefore the exact value of θ_- may be determined with little or no iteration once the product $\theta_-(1 + \epsilon)^{-1}$ is known. Equation (17) and expressions analogous to Eqs. (16) and (18) were also derived using the analytical relations for probe current (J) given by Kiel[12] and for $r/\lambda_- > 5$ the corresponding values of ϵ were found to compare favorably with those shown in Fig. 4. Values of ϵ valid for ion current collection in the orbital motion limit (oml) are also included in Fig. 4 while $\epsilon = 0$ in the thin sheath limit (tsl). The dotted portions of the curves shown in the figures are arbitrary

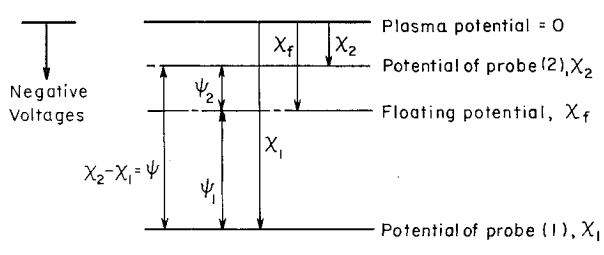

Fig. 3 Probe potential.

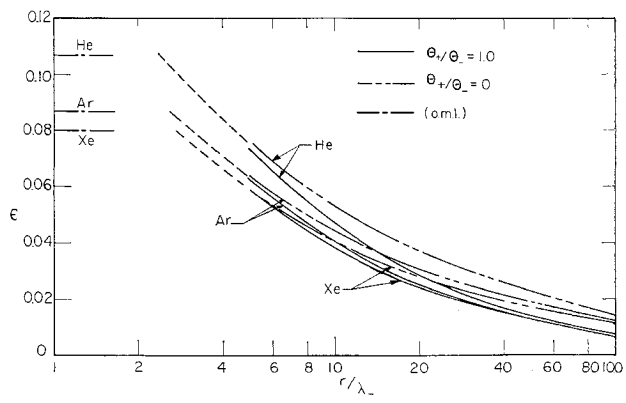

Fig. 4 Adjustment to electron temperature measurement.

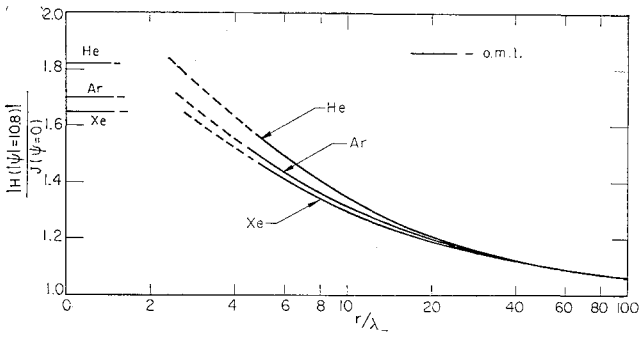

Fig. 5 Ratio of double-probe current to ion current.

extensions of the theoretical curves since the latter are valid only for $5 \leq r/\lambda_- \leq 100$ or in the oml or tsl.

Once the electron temperature is known the charged particle density may be computed from the magnitude of the double-probe current (H) measured at some large normalized potential ψ. In the limit of large ψ Eq. (13) reduces to the form

$$H(\psi) = J_{0*}(\beta + |\chi_*|)^\alpha = J_*(\chi_*) \tag{19}$$

where the asterisk signifies probe 1) or probe 2), whichever is appropriate. The number density is calculated from the expression

$$N = H(\psi)/[\theta_-^{1/2}(\beta + |\chi_f| + |\psi_*|)^\alpha A_*(|Z^3q^3|/2\pi M_+)^{1/2}] \tag{20}$$

where α, β, ψ_*, and χ_f are given by Eqs. (5, 6, 15, and 16), respectively. Because the measurement of $H(\psi)$ essentially yields the product $N(\beta + |\chi_f| + |\psi_*|)^\alpha$ and because α, ϵ, χ_f and ψ_* are weak functions of N, the solution of Eq. (20) requires some iteration. However for large negative potentials $I \ll J$ and in this limit $H(\psi)$ must be a measure of the single-probe ion current [see Eq. (19)]. If for example $J(\chi_* = \chi_f - 10)$ could be determined from the double-probe characteristic then the number density computation could proceed as described in Sec. 2. Examination of Eq. (15) reveals that for large values of potential ψ, ψ_* is a very weak function of the plasma properties. For example, it can be demonstrated that when $|\psi_*| = 10$ then $10.65 < |\psi| < 10.95$ for all values of $\theta_+/\theta_- \leq 1.0$, r/λ_-, and M_+/M_- provided $0.95 < A_2/A_1 < 1.05$. Since the variation of H within this small range of the normalized potential $|\psi|$ is always negligible compared to the experimental accuracy Eq. (19) may be written as

$$|H(\psi = \pm 10.8)| = J(\chi_f - 10) \tag{21}$$

Thus the absolute magnitude of the current in the double-probe circuit measured at $|\psi| = 10.8$ is equivalent to the ion current collected by a single-probe (whose area and radius are equal to that of the most negatively biased probe common to the double-probe) at a potential $\chi_f - 10$. As a result, the single-probe method illustrated by Sonin[6] and discussed in Sec. 2 may be applied directly for computations of N and r/λ_- from double-probe characteristics.

4. Interpretation of Double-probe Measurements

Some comment concerning the evaluation of the plasma properties from a typical double-probe characteristic such as that shown in Fig. 2 is in order.

Recall that Eq. (17) requires the evaluation of $J(V = 0)$. However, when $J = J(\psi)$ the ion current characteristic is obviously curved and straight line extrapolation of the double-probe characteristic (line S on Fig. 2) may introduce a significant error in the evaluation of $J(V = 0)$. Thus the initial computation of $\theta_-(1 + \epsilon)^{-1}$ will be incorrect. Fortunately, it turns out that a very accurate and rapid approximation for $J(V = 0)$ may be obtained by carefully fitting the entire characteristic between $10 \leq |\psi| \leq |\psi_{max}|$ where $|\psi_{max}| \gtrsim 35$ with a French curve and extrapolating along this curve to find the ion current at $\psi = 0$ (line F on Fig. 2). Because the true value of $J(\psi = 0)$ must be determined analytically after the ratio of probe radius to Debye length has been computed, theoretical values of $|H(\psi = \pm 10.8)|/J(\psi = 0)$ were determined from Eqs. (13) and (14) and are shown on Fig. 5 in order to provide a convenient subsequent check on the original estimate of $J(\psi = 0)$. The dependence of $|H(\psi = \pm 10.8)|/J(\psi = 0)$ on the relative energies θ_+/θ_- was found to be small and was therefore not included on Fig. 5. Again the dotted portions of the curves are arbitrary extrapolations.

Care should also be taken to evaluate the slope $(\partial H/\partial V)_{V=0}$ at the origin since the slope of $H(V)$ determined by the finite difference relation $[H(V) - H(-V)]/\Delta V$ centered about the $V = 0$ point on the characteristic, with $\Delta V = 2V$, is always $\leq (\partial H/\partial V)_{V=0}$, and hence the corresponding value of $\theta_-(1 + \epsilon)^{-1}$ thus obtained will be too large. Since in practice it is usually not possible to accurately interpret the slope of the characteristic within a region smaller than $\Delta V/\theta_- = \Delta\psi \leq 2.0$, this possible error in measurement must be considered. If $(\partial H/\partial V)_{V=0}$ cannot be measured, but instead, the slope of the characteristic is determined according to the finite difference relationship

$$(\partial H/\partial V)_{v=0 \text{ measured}} = [H(V_-) - H(-V_-)]/\Delta V \tag{22}$$

then it follows[13] from Eqs. (13, 14, and 17) that the resulting error in the electron temperature measurement is

$$\delta = [\theta_-(1 + \epsilon)^{-1}]_{\text{measured}}/[\theta_-(1 + \epsilon)^{-1}]_{\text{true}} = \psi(1 + \epsilon)(\beta - \chi_i)^\alpha(1 + \exp\psi)/2[(\beta - \chi_f + \psi_1)^\alpha(\exp\psi) - (\beta - \chi_f - \psi_2)\alpha] \tag{23}$$

provided $A_2 = A_1$. In the region of small ψ this expression is quite insensitive to changes in r/λ_-, θ_+/θ_-, and M_+/M_-, thus δ is given in Fig. 6 as a function of $\Delta\psi$ only. Therefore the error introduced by measuring the slope of the characteristic over some finite interval (around the point $V = 0$) as defined by Eq. (22) may easily be accounted for by reducing the measured value of $\theta_-(1 + \epsilon)^{-1}$ by appropriate factor of δ given in Fig. 6.

Using the proper values of $J_1(\psi = 0)$ and $J_2(\psi = 0)$ (which will be equal if $A_1 = A_2$) and the value of $(\partial H/\partial V)_{V=0}$, the computation of θ_-, r/λ_-, and N may proceed as follows. Compute $\theta_-(1 + \epsilon)^{-1}$ from Eq. (17). Use the equivalent of

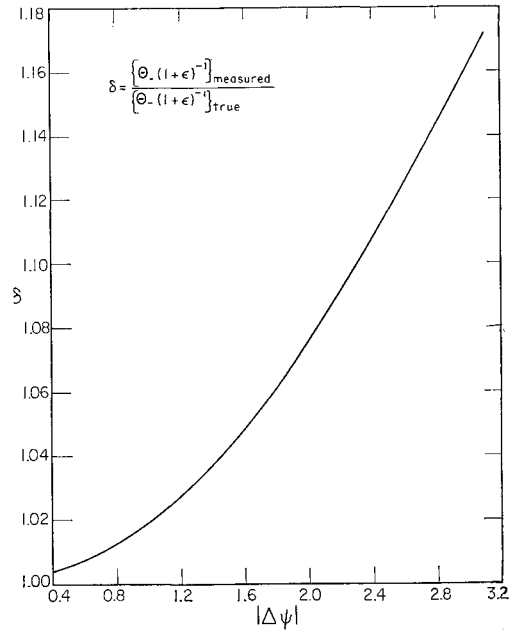

Fig. 6 Ratio of the actual slope of the double-probe characteristic to its measured value.

Sonin's[6] graphs [or Eq. (20) and the definition of Debye length] to compute N and r/λ_- based on the measured value of $|H|$ at a potential of $|\psi| = |V|/[\theta_-(1 + \epsilon)^{-1}] = 10.8$. Then evaluate ϵ from Fig. 4 and compute θ_-. Repeat the preceding computations of N, r/λ_-, ϵ, and θ_-, each time using the latest value of θ_-, and the value of $|H|$ now measured at $|\psi| = |V/\theta_-| = 10.8$, until self-consistent values for these quantities are obtained. Use this value of r/λ_- to compare the measured ratio of $|H(\psi = \pm 10.8)|/J(\psi = 0)$ with the theoretical value given in Fig. 5. If the measured and theoretical values agree the problem is solved since θ_-, r/λ_-, and N have been determined. If the values are inconsistent the theoretical value should be used to provide a new estimate of $J_1(\psi = 0)$ and $J_2(\psi = 0)$ and the iteration procedure previously described must be repeated. Because ϵ is always small and because the French curve interpolation of H provides quite accurate values for $J_1(\psi = 0)$ and $J_2(\psi = 0)$, the iteration procedure is always short; with some practice the plasma properties may be determined directly from the double-probe characteristic. For example consider the measurement of the plasma properties from the characteristic shown in Fig. 2. The procedure described previously immediately yields the correct values of $\theta_- = 0.20$, $r/\lambda_- = 5.0$ and $[J(\psi = 0)]_{\text{estimated}}/[J(\psi = 0)]_{\text{theoretical}} = 1.0$. In contrast, straight line interpolation of the ion characteristic initially yields $\theta_- \approx 0.25$, $r/\lambda_- \sim 4.1$ and $[J(\psi = 0)]_{\text{estimated}}/[J(\psi = 0)]_{\text{theoretical}} = 1.23$. Thus additional iteration must be used to properly evaluate $J(\psi = 0)$, θ_-, r/λ_- and N. If straight line interpolation were used and if in addition $(\partial H/\partial V)_{V=0}$ were taken as the slope measured over the region $\Delta\psi = 2.0$ (e.g., $-0.2 \leq V \leq 0.2$ on Fig. 2) according to Eq. (22), then the incorrect value for electron temperature of 0.27 would be obtained. The error arising in the computation of $\theta_-(1 + \epsilon)^{-1}$, which results from the incorrect measurement of $(\partial H/\partial V)_{V=0}$, should be corrected using the values of δ presented in Fig. 6 before starting any iteration procedure.

The methods described above have been used successfully (see Refs. 11, 15, and 16) to obtain measurements of the plasma properties (N and θ_-) from the double-probe characteristics which are consistent with those values computed from the single-probe characteristics.

5. Conclusions

An algebraic relation describing the single-probe current-voltage characteristic in the region where the current attracted to the probe is potential dependent has been presented. The analogous double-probe characteristics were also described in analytical form. In addition, equations were derived and methods were discussed for determining both electron temperature and charged particle density from the double-probe characteristics. In particular, these results have been presented in order to provide a useful tool to those who use probes for diagnostic purposes.

References

[1] Loeb, L. B., *Basic Process of Gaseous Electronics*, University of California Press, Berkeley and Los Angeles, Calif., 1955.

[2] deLeeuw, J. H., "Electrostatic Plasma Probes," *Physico-Chemical Diagnostics of Plasmas*, edited by T. P. Anderson et al., Northwestern Univ. Press, Evanston, Ill., 1963, p. 65.

[3] Chen, F. F., "Numerical Computations for Ion Probe Characteristics in a Collisionless Plasma," *Plasma Physics* (*Journal of Nuclear Energy*, Part C) Vol. 7, 1965, p. 47.

[4] Laframboise, J. G., "Theory of Spherical and Cylindrical Langmuir Probes in a Collisionless, Maxwellian Plasma at Rest," Rept. 100, 1966, University of Toronto Institute for Aerospace Studies; see also *Rarefied Gas Dynamics*, Vol. 2, edited by J. H. deLeeuw, Academic Press, New York, 1966, p. 22.

[5] Bernstein, I. B. and Rabinowitz, I. N., "Theory of Electrostatic Probes in a Low Density Plasma," *The Physics of Fluids*, Vol. 2, 1959, p. 112.

[6] Sonin, A. A., "Free-Molecule Langmuir Probe and Its Use in Flowfield Studies," *AIAA Journal*, Vol. 4, No. 9, Oct. 1966, p. 1588.

[7] Chen, F. F., Etievant, C., and Mosher, D., "Measurement of Low Plasma Densities in a Magnetic Field," *The Physics of Fluids*, Vol. 2, 1968, p. 811.

[8] Dunn, M. G. and Lordi, J. A., "Measurement of Electron Temperature and Number Density in Shock Tunnel Flows. Part I, Development of Free-Molecular Langmuir Probes," *AIAA Journal*, Vol. 7, No. 8, Aug. 1969, p. 1458.

[9] Graf, K. A. and deLeeuw, J. H., "Comparison of Langmuir Probe and Microwave Diagnostic Techniques," *Journal of Applied Physics*, Vol. 38, 1967, p. 4466.

[10] Johnson, E. O. and Malter, L., "A Floating Double Probe Method for Measurements in Gas Discharges," *Physics Review*, Vol. 80, 1960, p. 58.

[11] Peterson, E. W. and Talbot, L., "Langmuir Probe Response in a Turbulent Plasma," AIAA Paper 69-698, San Francisco, Calif., 1969.

[12] Kiel, R. E., "Electrostatic Probe Theory for Free Molecule Cylinders," *AIAA Journal*, Vol. 6, No. 4, April 1968, p. 708.

[13] Peterson, E. W. and Talbot, L., "An Analytical Description of the Free-Molecule Cylindrical Electrostatic Single-Probe and Double-Probe Measurements," Aeronautical Sciences Division Rept. AS-69-12, 1969, Univ. of California, Berkeley.

[14] Langmuir, I. and Mott-Smith, H. M., "The Theory of Collectors in Gaseous Discharges," *Physics Review*, Vol. 28, 1962, p. 727.

[15] Kirchhoff, R. H., Peterson, E. W., and Talbot, L., "An Experimental Study of the Cylindrical Langmuir Probe Response in the Transition Regime," AIAA Paper 70-85, New York, 1970.

[16] Kirchhoff, R. H. and Talbot, L., "An Experimental Study of the Shock Structure in a Partially Ionized Gas," AIAA Paper 64-697, San Francisco, Calif., 1969.